Final Report
for Subcontract 9-XC3-Y9148-1
Research Activities in Modeling the Selective Oxidation of Hydrocarbons

Anthony K. Rappé
Department of Chemistry
Colorado State University

The selective oxidation of organic substrates by oxygen wherein all four oxidizing equivalents are used productively remains an unsolved problem in catalysis. Even nature does not provide a solution to this problem, enzymes such as methane monooxygenase and cyctochrome P450 waste one of the oxygen atoms of O_2 by generating an equivalent of water for each equivalent of substrate oxidized. In collaboration with Sergio Gorun at Exxon an idealized catalytic cycle that could solve this problem has been devised and is given in scheme 1. Three separate, important steps are involved. First O_2 must be rapidly bound, then the O-O bond must be cleaved, and finally each oxo ligand needs to react independently with the substrate ultimately regenerating the resting catalyst. The first and last steps were investigated as a part of this research program. Molecular mechanics was used to investigate the O_2 binding step and *ab initio* electronic structure tools were used to study M-O bonding and the reactivity of M=O bonds with methane.

During the course of developing models for the water oxidizing catalyst of photosystem II[3] (and the microscopic reverse O_2 cleavage reaction) an interesting structural feature of μ,η^2-peroxides was uncovered and subsequently investigated by molecular mechanics. The molecular mechanics minimized geometries for a pair of triply bridged, octahedral Mn complexes with μ-oxo and μ-formato bridges as well as the μ,η^2-peroxide bridge were found, by molecular mechanics with the UFF force field, to contain peroxo bridges with substantially twisted peroxide linkages (Mn-O-O-Mn dihedral (ϕ) angles of 56° and 59°). In order to confirm that this was not an artifact of the UFF force field, the geometry for the cationic portion of [(1,4,7-triazacyclononane)$_2$ $Mn_2(O)_2(O_2)](ClO_4)_2$, was determined by molecular mechanics. The resulting molecular mechanics Mn-O-O-Mn ϕ angle of 5.6° was in reasonable accord with the angle of 3.1° found in the crystal structure. This agreement suggested that the force field structures found were reasonable and that the M-O-O-M ϕ angle could possibly be controlled by the nature of the auxilary bridging ligands.

Control of the M-O-O-M dihedral angle has ramifications for the facile, reversible addition of O_2 to a dinuclear metal site, the first step in the hypothetical catalytic cycle in scheme 1. The perpendicular orientation of the two singly occupied π^* orbitals of O_2 suggests that a least motion addition (elimination) pathway of O_2 would form/(come from) a dinuclear complex with a M-O-O-M ϕ angle near 90°.

A survey of the 31 μ,η^2-peroxide structures in the Cambridge structural data base yielded 17 singly bridged structures (all with M-O-O-M ϕ angles greater than 90° and 14 with M-O-O-M ϕ angles greater than 140°), 13 doubly bridged structures (9 with M-O-O-M angles between 50° and 70°), and one triply bridged structure, with a M-O-O-M angle of 3° (the Mn complex discussed above). This data is collected in Table 1.

Given the range of ϕ crystallographically observed, a structural source for the preferred M-O-O-M twist angle was sought. The UFF force field was used to investigate the dependence of ϕ on Mn-Mn distance for a four-membered ring model consisting of two Mn atoms and two O atoms (the Mn's connected to simulate the Mn octahedral coordination environment). For each

constrained Mn-Mn distance the remaining degrees of freedom were optimized. As would be expected (based on simple geometry) small Mn-Mn distances resulted in small ϕ and large Mn-Mn distances resulted in large ϕ. In the limit of the Mn's coalescing the resulting triatomic must be coplanar and in the limit of very large Mn-Mn the Mn-O-O-Mn unit must be stretched into a line. For Mn-Mn distances less than 2.7 Å the model suggests a ϕ of 0°. For Mn-Mn distances greater than 4.1 Å the model suggests a ϕ of 180°. In between the small R and large R limits the UFF potential curve follows a monotonic, near linear behavior as shown by the dashed line in Figure 1. The 28 experimental ϕ-R pairs for μ,η^2-peroxo complexes are plotted as filled triangles. The three structures with μ,η^2-superoxo bridges are plotted as gray triangles in Figure 1. The μ-oxo bridges in **3** were sequentially replaced by acetate bridges to assess the impact that bridge structure has on ϕ. These structures are displayed as filled squares in Figure 1. Finally, O_2 was bound to several metal oxide surfaces, the resulting ϕ-R pairs are plotted as open squares in Figure 1.

Since the UFF structures of isolated molecules, surface bound species, and the model curve were found to be consistent with the available experimental structures an analysis of the individual terms in the molecular mechanics energy expression was carried out. The torsional energy as a function of Mn-Mn distance is plotted in Figure 2. A conclusion that can be drawn is that complexes with Mn-Mn distances near 3.5 Å should have little torsional strain and favor reversible O_2 complex formation elimination.

This molecular modeling study provides a simple critera for the construction of dinuclear complexes capable of binding O_2 with a low barrier. Once O_2 is bound it must be cleaved and then the individual M-O units reacted with hydrocarbon. In general, the bonding between metal centers and oxygen ligands follows the general pattern of organic chemistry with triple bonds (analogous to CO), double bonds (analogous to formaldehyde), resonant radicals (analogous to dioxygen), radicals (analogous to hydroxy radical), and polar covalent single bonds (analogous to water). To systematically develop an understanding of the reactivity of methane (to form methanol) with M-O linkages one must react methane with the differing bonding modes accessible to M-O linkages. We began by picking two metal complexes with terminal M-O linkages, one a model of a MO_3 111 surface and the other a model of a Fe_2O_3 100 surface, and initiated a study characterizing the transition state and exothermicity of the reaction for L_nM-O + methane to form the addition complex $L_nMOH(CH_3)$. The first case $(OH)_2CrO_2$, a model for a MO_3 111 surface, represents a complex with a formaldehyde-like M-O double bond. Even though this metal complex is diamagnetic there is indirect experimental evidence that it reacts with alkanes as though it were a radical. Though the reaction could occur through a concerted addition pathway with the formed alkyl product being unstable to homolysis. It was thought that characterization of the reaction coordinate, with MESA, for this reaction would help refine our knowledge of the reaction of methane with M=O complexes. Unfortunately we found that the alkyl product $(OH)_2CrOH(CH_3)$ was unstable to loss of CH_3OH or CH_3 at the Hartree Fock (HF) level and it is clear from the published work of Cundari and the completed work of Hay, Martin, et. al. that electron correlation

is essential in describing M=O systems. At the Hartree-Fock wavefunction level the M=O bond distances are rather dramatically unestimated (> 0.06Å). This error undoubtedly carries over to energetic estimates and reaction exothermicities. If a reaction proceeds from a molecule with a M-O double bond to a molecule with a M-O single bond the differential error associated with the π bond will cause the transition state for the reaction to be improperly placed along the reaction coordinate. For Cl_2CrO_2 dissociating to $CrCl_2$ and O_2, a Hartree Fock wavefunction suggests that the reaction is exothermic when in fact it is more than 100 kcal/mol endothermic. This more than 100 kcal/mol bias in the Hartree Fock potential surface has caused the potential surface for reaction of CH_4 with Cl_2CrO_2 to be quite unstable. For example the reaction given in equation (1) should be endothermic, but using a Hartree Fock wavefunction it is not. This error causes virtually any estimate of the transition state for addition of methane across a M=O π bond to lead instead to direct elimination of methanol (which is certainly not correct).

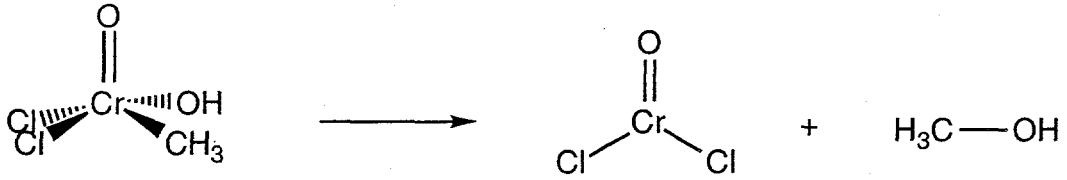

In order to minimize this energetic error we have begun a systematic study of the molecules $Cl_2Ti=O$, $Cl_3V=O$, and Cl_2CrO_2 to see if a CAS wavefunction will correctly describe the molecular geometry and if a CAS+SD CI wavefunction will approximately describe the reaction energetics for M=O bond cleavage (the structures and reaction energetics are known for $Cl_3V=O$, and Cl_2CrO_2). Results for VCl_3O are collected in Tables 2 and 3. The HF error in V=O bond distance is corrected by either a CAS wavefunction or a MP2 calculation (V-O in $VO(OR)_3$ compounds is ~1.58 Å). It appears as though the CAS wavefunction provides the best estimate of vibrational frequencies. This work will continue into the future.

The second metal complex studied by *ab initio* methodologies was a dinuclear Iron(III) complex with a terminal oxo ligand, a model of the 100 surface of hematite (Fe_2O_3). The model complex (with differing ligands) was thought to afford knowledge about M=O linkages as well as O_2 like resonating systems as well as O radical like systems. A geometry optimization was carried out for the first of these complexes. The ground state singlet, a low lying triplet on to the ten electron high spin state of the dinuclear Fe(III) complex model (with a terminal oxo ligand) have been characterized as having a common underlying electronic structure. The iron bound to the terminal oxo ligand is best characterized as being a high spin Fe(II) center, the other iron is high spin Fe(III) and the oxo has "O2"-like oxygen character, that is the oxo group has one singly occupied p-pi orbital and one doubly occupied p-pi orbital. These two p-pi orbitals have companion orbitals on the Fe(II) center--the singly occupied oxo p-pi orbital is parallel with a doubly occupied d-pi orbital on the Fe(II), the doubly occupied oxo p-pi orbital is parallel to a singly occupied d-pi orbital on the Fe(II) center. Given the near four-fold nature of the octahedral coordination environment at the Fe(II) center there should be a resonance interaction with a

configuration of the Fe(II)-O unit where the singly and doubly occupied orbitals exchange position. The "O_2"-like nature of the bonding should prevent this unit from acting like a radical abstracting center though a comparitive study of the reaction of O_2 with methane and the dinuclear iron system with methane needs to be carried out to first test the accuracy of the methodology (previous work with O_2 has been carried out) and to set up a comparison between the two 'oxo' type systems. This work is ongoing.

References

1. Theoretical modeling of the mechanism of dioxygen activation and evolution by tetranuclear manganese complexes D. M. Proserpio, A. K. Rappé, and S. M. Gorun Inorg. Chim. Acta, *213*, 319 (1993).
20. U. Thewalt Z. Anorg. Allg. Chem., *393*, 1, 1972.
21. F. Bigoli, M. Lanfranchi, E. Leporati, M. A. Pellinghelli Cryst.Struct.Commun., *10*, 1445, 1981.
22. M. Suzuki, I. Ueda, H. Kanatomi, I. Murase Chem.Lett., *185*, 1983.
23. D. D. Dexter, C. N. Sutherby, M. W. Grieb, R. C. Beaumont, Inorg. Chim. Acta, *86*, 19, 1984.
24. S. Fallab, M. Zehnder Helv. Chim. Acta, *67*, 392, 1984.
25. J. Springborg, M. Zehnder Helv. Chim. Acta, *69*, 199, 1986.
26. M. Calligaris, G. Nardin, L. Randaccio, A. Ripamonti J. Chem. Soc. A, *1069*, 1970.
27. G. J. Gainsford, W. G. Jackson, A. M. Sargeson Aust. J. Chem., *39*, 1331, 1986
28. U. Thewalt, G. Struckmeier, Z. Anorg. Allg. Chem. *419*, 163, 1976.
29. I. B. Baranovskii, A. N. Zhilyaev, L. M. Dikareva, A. V. Rotov,Zh.Neorg.Khim., *31*, 2892, 1986.
30. R. R. Jacobson, Z. Tyeklar, A. Farocq, K. D. Karlin, Shuncheng Liu, J .Zubieta J. Am. Chem. Soc., *110*, 3690, 1988.
31. E. Bouwman, W. L. Driessen, J. Am. Chem. Soc. *110*, 4440, 1988.
32. H. Macke, M. Zehnder, U. Thewalt, S. Fallab, Helv. Chim. Acta *62*, 1804, 1979.
33. B. A. Vaartstra, Jianliang Xiao, M. Cowie, J. Am. Chem. Soc. *112*, 9425, 1990.
34. L. M. Dikareva, V. I. Andrianov, A. N. Zhilyaev, I. B. Baranovskii, M. A. Porai-Koshits, Zh. Neorg. Khim. *33*, 960, 1988.
35. P. V. Bernhardt, G. A. Lawrance, T. W. Hambley J. Chem. Soc., Dalton Trans., *235*, 1990.
36. N. F. Curtis, W. T. Robinson, D. C. Weatherburn, Aust. J. Chem. *45*, 1663, 1992.
37. M. Zehnder, U. Thewalt, Z. Anorg. Allg. Chem. *461*, 53, 1980.
38. J. R. Fritch, G. G. Christoph, W. P. Schaefer Inorg. Chem., *12*, 2170, 1973.

39. M. Zehnder, U. Thewalt, S. Fallab, Helv. Chim. Acta *62*, 2099, 1979.
40. J. H. Timmons, A. Clearfield, A. E. Martell, R. H. Niswander Inorg. Chem., *18*, 1042, 1979.
41. L. A. Lindblom, W. P. Schaefer, R. E. Marsh Acta Crystallogr., Sect. B, *27*, 1461, 1971.
42. S. Fallab, M. Zehnder, U. Thewalt, Helv. Chim. Acta, *63*, 1491, 1980.
43. I. V. Kuz'menko, A. N. Zhilyaev, M. A. Porai-Koshits, I. B. Barabovskii Zh. Neorg. Khim., *35*, 1150, 1990.
44. U. Thewalt, R. E. Marsh Inorg. Chem., *11*, 351, 1972.
45. S. Bhaduri, L. Casella, R. Ugo, P. R. Raithby, C. Zuccaro, M. B. Hursthouse J. Chem. Soc., Dalton Trans., *1624* , 1979.
46. U. Bossek, T. Weyhermuller, K. Wieghardt, B. Nuber, J. Weiss J. Am. Chem. Soc., *112*, 6387, 1990.
47. Yu. A. Simonov, A. A. Dvorkin, A. P. Gulia, A. N. Sobolev, O. A. Bologa, D. I. Gredinaru, N. V. Gerbeleu, T. I. Malinovskii Dokl. Akad. Nauk SSSR, *305*, 635, 1989.
48. B. M. Gatehouse, G. McLachlan, L. L. Martin, R. L. Martin, L. Spiccia Aust. J. Chem., *44*, 351, 1991.
49. T. Shibahara, S. Koda, M. Mori Bull. Chem. Soc. Jpn., *46*, 2070, 1973.
50. J. H. Timmons, R. H. Niswander, A. Clearfield, A. E. Martell Inorg. Chem., *18*, 2977, 1979.
51. M. Zehnder, U. Thewalt, S. Fallab Helv. Chim. Acta, *59*, 2290, 1976.

Table 1

CSD Name	Ref.	Compound	M-O-O-M ϕ(°)	M-M R (Å)
APENCT	20	μ^2-Amido-μ^2-peroxo-bis(bis(ethylenediamine)cobalt(iii)) tri-thiocyanate monohydrate	-62.58	3.28
BATTAR	21	ae,cd,hk,ij-tetrakis(Ethylenediamine)-f-(μ^2-hydroxo)-bg-(μ^2-peroxo)-di-cobalt(iii) tri-iodide hydrate	-54.61	3.23
BUMVUA	22	(μ^2-Benzoato)-(μ^2-dioxygen)-(μ^2-2,6-bis(bis(2-pyridylmethyl)-aminomethyl)-4-methylphenolato)-di-cobalt bis(tetrafluoroborate) dihydrate		
COFYIF	23	(μ^2-Superoxo) bis((diethylenetriamine) (ethylenediamine)-cobalt(iii)) diperch lorate trichloride dihydrate	180	4.55
COTXIS	24	(μ^2-Peroxo)-bis(tris(2-aminoethyl)amine-cyano-cobalt(iii)) diperchlorate	180	4.60
DODVIB	25	meso-cdelta,clambda-(μ!2$-Peroxo)-($\mu^2$-hydroxo)-bis(bis(ethylenediamine)-rhodium(iii)) tris(trifluoromethanesulfonate) dihydrate	-68.74	3.45
DOESCF10	26	μ^2-Di-oxygen-bis(N,N'-ethylene-bis(salicylideneiminato)-(dimethyl formamide-O)-cobalt(ii))	-110.11	4.24
DUTCOK	27	p,p-(μ^2-Peroxo)-bis((tris(2-aminoethyl)-amine-N,N',N'',N''')-bis(ethylglycinate-N)-cobalt(iii)) tetraperchlorate	180	4.62
ENCOXT	28	μ^2-Hydroxo-μ^2-peroxo-bis(bis(ethylenediamine) cobalt(iii)) dithionate nitrate dihydrate	60.89	3.28
ENSXCO	28	μ-Hydroxo-μ-superoxo-bis(bis(ethylenediamine) cobalt(iii)) tetranitrate monohydrate	-21.94	3.26
FINBUZ	29	Diaqua-(μ^2-peroxo)-(μ^2-hydroxo)-hexakis(pyridyl)-di-rhodium triperchloratedihydrate	62.72	3.44
GECRAH	30	(μ^2-Peroxo-O,O')-bis(tris(((2-pyridyl)methyl)amine-N,N',N'',N''')-copper(ii)) bis(hexafluorophosphate) diethyl ether solvate	180	4.36
GETRAY	31	(μ^2-Hydroxo)-(μ^2-peroxo)-bis(1,6-bis(5-methyl-4-imidazolyl)-2,5-dithiahexane-N,N',S,S')-di-cobalt(iii) trinitrate	-60.14	3.24
HPZDCO	32	(μ^2-Hydroxo)-(μ^2-peroxo)-bis(4,7-dimethyl-1,4,7,10-tetra-azadecane-cobalt(iii)) triperchlorate dihydrate	-68.31	3.32
JIHDIN	33	(μ^2-Peroxo)-dicarbonyl-di-iodo-bis(μ^2-bis(diphenylphosphino)methane-P,P')-	-33.97	2.71

Table 2
VCl_3O Geometry

Geometric Variable	HF	CAS(6,6)	MP2
V-O	1.508	1.576	1.602
V-Cl	2.154	2.194	2.23
O-V-Cl	108.3	104.6	104.1
Cl-V-Cl	110.6	113.8	114.2

Table 3
Vibrational Frequencies

Mode	HF	CAS	MP2	exp.
e	128.3	113.0	121.6 (121.8)	129
a1	175.7	165.5	157.4	165
e	276.5	259.4	274.8 (275.2)	249
a1	408.9	379.7	365.4	408
e	499.0	473.8	453.0 (455.1)	504
a1	1285.3	1047.4	2054.0	1035

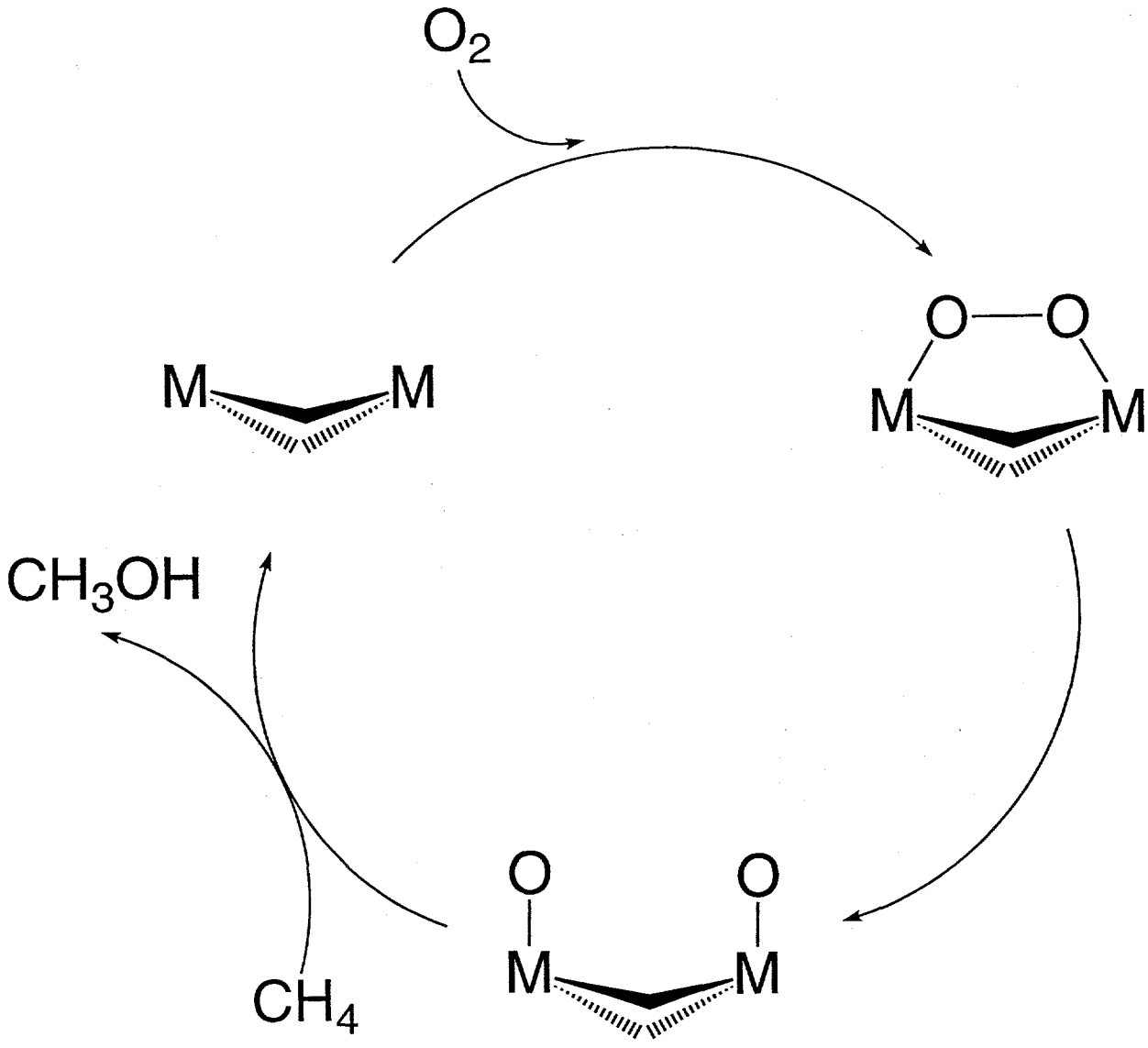

Scheme 1

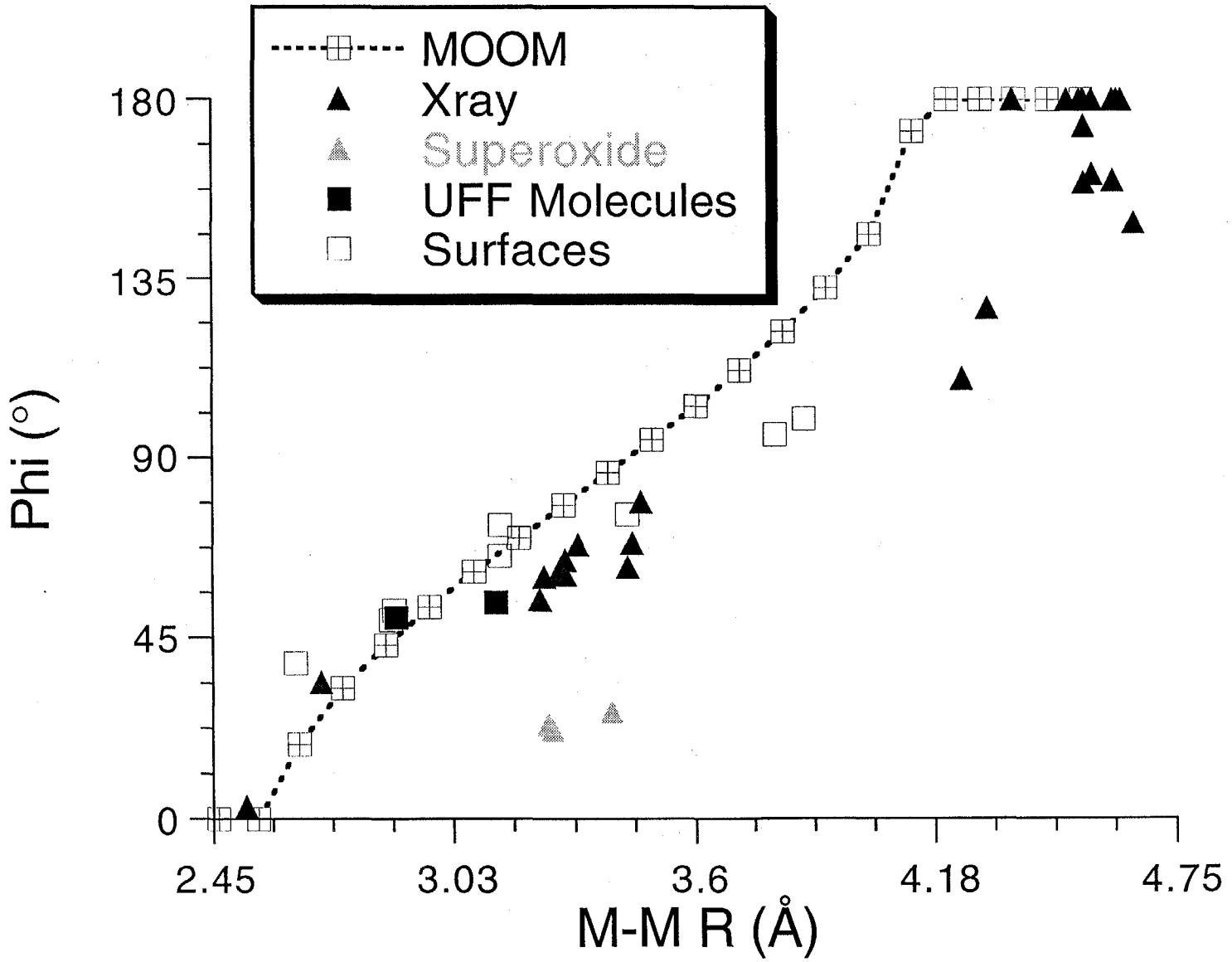
MOOM
Xray
Superoxide
UFF Molecules
Surfaces
180
135
90
45
0
Phi (°)
2.45
3.03
3.6
4.18
4.75
M-M R (Å)

Figure 1

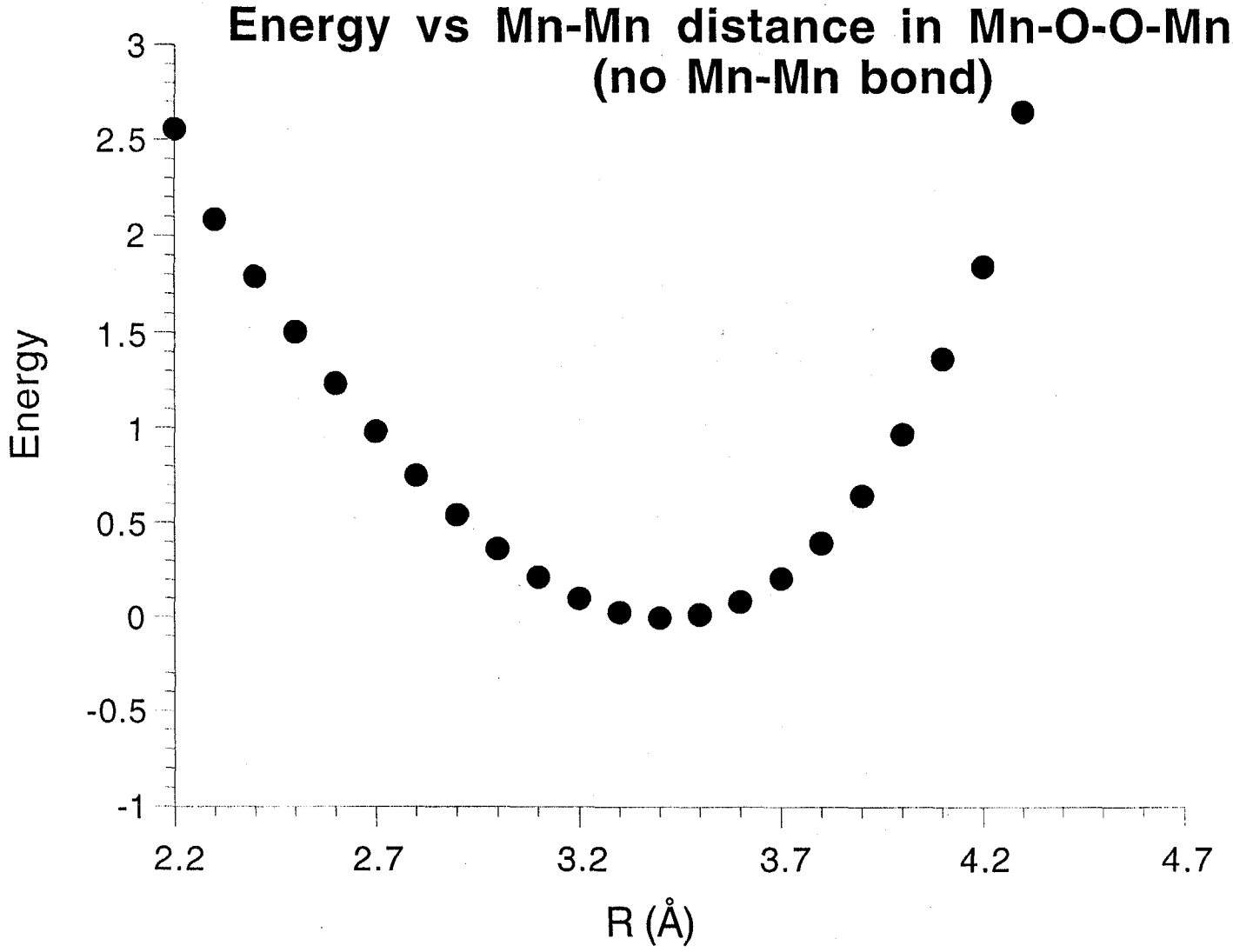
Energy vs Mn-Mn distance in Mn-O-O-Mn
(no Mn-Mn bond)
Energy
3
2.5
2
1.5
1
0.5
0
-0.5
-1
2.2
2.7
3.2
3.7
4.2
4.7
R (Å)

Figure 2